applied sciences

MDPI

Communication

Variation of Acoustic Transmission Spectrum during the Muscle Fatigue Process

Pan Li [1], Guanjun Yin [2,*], Shibo Nie [1] and Jianzhong Guo [1,*]

[1] School of Physics and Information Technology, Shaanxi Normal University, Xi'an 710119, China
[2] Key Laboratory of Modern Teaching Technology, Shaanxi Normal University, Xi'an 710062, China
* Correspondence: yinchamp@snnu.edu.cn (G.Y.); guojz@snnu.edu.cn (J.G.)

Abstract: The timely assessment of muscle fatigue makes sense for reducing the risk of musculoskeletal injury during exercise. In general, muscle fatigue is accompanied by physiological changes. These changes affect the acoustic transmission properties of the skeletal muscles. This study investigated the variation of the acoustic transmission spectrum (ATS) of human upper arm muscles during sustained static contractions (SC). Based on the B-ultrasound image and radiofrequency (RF) ultrasonic echoes, we abstracted the RF echo signals from the subcutaneous fatty/fascia (SFF) and deep fascia/bone (DFB) interfaces. By dividing the echo spectrum of the DFB by the spectrum of the SFF, we obtained the ATS of the upper arm muscles. Then, by fitting the ATS with both the linear function ($A(f) = af + b$) and power-law function ($A(f) = \alpha f^{\beta}$), we analyzed the variations of a, b, α, and β along with the SC process of skeletal muscle. As muscle fatigue increases, the slope a decreases and the intercept b increases linearly; the α increases exponentially and β decreases linearly. In addition, the variation magnitude of ATS relates to the maximum voluntary contraction (MVC) force and the strength of the SC motion. These results suggest that a comprehensive analysis of ATS is a potential metric for assessing muscle fatigue.

Keywords: muscle fatigue; acoustic transmission spectrum; RF ultrasonic echo; static contraction

check for updates

Citation: Li, P.; Yin, G.; Nie, S.; Guo, J. Variation of Acoustic Transmission Spectrum during the Muscle Fatigue Process. *Appl. Sci.* **2023**, *13*, 947. https://doi.org/10.3390/app13020947

Academic Editors: Arkady Voloshin and Anthony William Coleman

Received: 25 November 2022
Revised: 24 December 2022
Accepted: 9 January 2023
Published: 10 January 2023

Copyright: © 2023 by the authors. Licensee MDPI, Basel, Switzerland. This article is an open access article distributed under the terms and conditions of the Creative Commons Attribution (CC BY) license (https://creativecommons.org/licenses/by/4.0/).

1. Introduction

Muscle fatigue is generally manifested as the decrease in peak force, velocity, and power in response to contractile activity [1]. The mechanisms of muscle fatigue mainly involve neurophysiology, cell metabolism, and fiber morphology changes [2–4]. Sustained exercises can result in a decrease in the ability to generate voluntary force [3] and an increase in the fatigue state [5]. Moreover, overtraining under excessive fatigue can significantly increase the risk of musculoskeletal injury [6]. The timely assessment of muscle fatigue is valuable for reducing the additional injury risk during exercise, especially for people with prolonged or intense workout sessions [7].

The mainstream methods for assessing muscle fatigue include the perceived exertion rating scale, the blood index, surface electromyography (sEMG), and ultrasound imaging [8–11]. The perceived exertion rating scale depends on subjective individual feelings, which lack objectivity [8]. The blood biochemical is a gold standard, while its invasiveness and non-real-time are the main limitations [9]. sEMG is a timely and noninvasive physical method, but it is susceptible to various factors, especially electromagnetic interferences from other devices or the environment [10]. B-ultrasound imaging can visualize the muscle structure in real time by reconstructing the original ultrasonic echoes scattered and reflected by the impedance-changing interface [11]. Ultrasound images perform well in analyzing the changes in the muscular architectural characteristics (the muscle thickness, pennate angle, and fascicle length) [12,13] and the textural features (the ultrasonic image entropy and echo intensity) [14,15] during muscle fatigue.

However, in addition to muscle structural information, the radiofrequency (RF) ultrasonic echo signals also carry physiological information about the muscle tissue [16].

Sustained exercise can induce muscle fatigue as well as relevant changes in the physiological conditions of muscle [17,18], such as myofibrillar disruptions [19], metabolite [3] and interstitial fluid concentration increases [20]. The spectrum of RF signals relates to the information about the size, concentration, and acoustic impedance of the scatterers [21,22], which is effective in evaluating tissue changes [23–25]. Therefore, the acoustic transmission spectrum (ATS) can reflect physiological changes in skeletal muscle and is potentially an effective indicator for assessing muscle fatigue.

In this study, we investigated variations of ATS in human upper arm muscle fatigue. We acquired the RF signals and B-ultrasound images during the static contraction (SC) of the upper arm muscles of nine healthy male volunteers. We abstracted the RF signals reflected from the subcutaneous fatty/fascia (SFF) and deep fascia/bone (DFB) interfaces, respectively. The ATS of the skeletal muscle was calculated by dividing the echo spectrum of the DFB by the SFF spectrum. Then, we fitted the ATS with linear function ($A(f) = af + b$) and power-law function ($A(f) = \alpha f^{\beta}$) and analyzed variations of a, b, α, and β along with the SC of skeletal muscle.

2. Materials and Methods

2.1. Experimental Setups

2.1.1. Subjects

This study recruited nine healthy male volunteers (age: 25 $\pm$ 3 years, height: 175 $\pm$ 5 cm, weight: 72 $\pm$ 8 kg). None of them had experienced an upper-arm injury or strenuous exercise during the week prior to the trial. We selected the muscles of their dominant upper arms as the samples for the experiment. The volunteers warmed up lightly to familiarize themselves with the procedure and avoid injury during the experiment. Each volunteer learned the essentials of the experiment and signed a written informed consent form.

2.1.2. Instruments

A multi-channel ultrasound system (Vantage 256, Verasonics Inc., Kirkland, WA, USA) and a linear array transducer (128 elements, L11-5v, Verasonics) with a central frequency of 7.8 MHz were used to acquire the ultrasonic B-mode images and RF signals. The image depth was 5 cm, and the width was 4 cm. The sampling frequency was 31.25 MHz. The system settings, such as the time gain compensation and focal depth, were kept constant in the experiment.

2.1.3. Exercise Protocol

First, the maximum voluntary contractions (MVC) force of each volunteer was measured by three MVC tests with at least 15 min rests. Then, each volunteer was asked to perform a sub-maximal (60% MVC force) sustained SC until exhaustion. For the SC procedure, the volunteer sits in a chair and holds a dumbbell with the elbow angle remaining at 90 degrees. The subject was verbally encouraged to keep the position as long as possible. The test was stopped when the upper arm began to tremble, to avoid measurement errors from muscle tremors. The array transducer was fixed to the upper arm parallel to the muscle fibers, and its center was placed at the thickest part of the muscle. B-ultrasound images and RF signals were acquired every 5 s. The maximum endurance time (MET) [26] of each test was recorded.

2.2. Data Analysis

2.2.1. Calculation Procedure

Figure 1 shows the calculation procedure for the ATS of the skeletal muscles used in this study. Due to the big difference in acoustic impedance [26], the interfaces of SFF and DFB are evident and distinguishable in the B-ultrasound images, as shown in Figure 1a. According to their depths, the corresponding echoes of SFF and DFB can be abstracted from the RF ultrasonic signals, as shown in Figure 1b. Echoes of SFF path through the skin and fatty layers, and echoes of DFB path through the skin, fatty, and skeletal muscle (biceps

brachii, brachialis) layers. In contrast to the echoes of SFF, the echoes of DFB additionally carry the acoustic transmission properties of the skeletal muscles. The echo signal of each channel is multiplied by a Hamming window of length L (L = length of echoes) to suppress spectral lobes, and the spectrum is obtained by fast Fourier-transform (FFT).

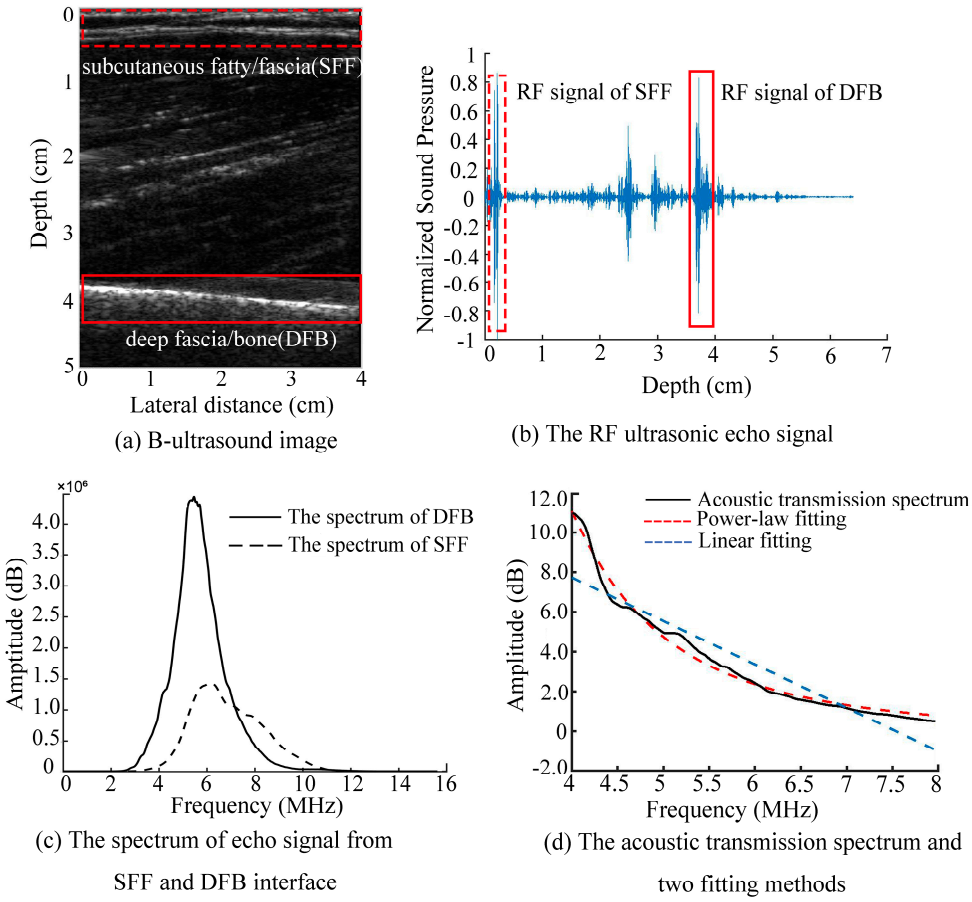


Figure 1. Procedure of data analysis for the acoustic transmission spectrum.

Due to the inhomogeneity of the muscle tissue [27], the spectrums of the DFB echoes are different from the echo spectrums of SFF, as shown in Figure 1c. In order to eliminate the spectrum effects of the ultrasound system, the ATS of the skeletal muscle is calculated by dividing the echo spectrums of the DFB by that of SFF. We averaged the ATS of 128 channels to further reduce the measurement errors. In this work, the spectrum analysis range is chosen similarly to the bandwidth of the ultrasound system (4–8 MHz) to ensure an acceptable signal-to-noise ratio.

2.2.2. Fitting Models

The linear fit is frequently employed to analyze the ultrasonic spectrum [28], while the acoustic attenuation in the muscle tissue obeys the power-law function in the frequency domain [29]. Therefore, we fitted the ATS with both linear function ($A(f) = af + b$) and power-law function ($A(f) = \alpha f^{\beta}$), as shown in Figure 1d. Figure 2 shows the ATSs of volunteer 1 every 5 s during the SC process. For each subject, the regression coefficients were between 0.79 and 0.95 for the linear fit and between 0.94 and 0.99 for the power law fit. The results suggest that a power-law model is more appropriate for the ATS analysis. While the linear and power-law models represent specific physical laws, their coefficients have distinct physical meanings.

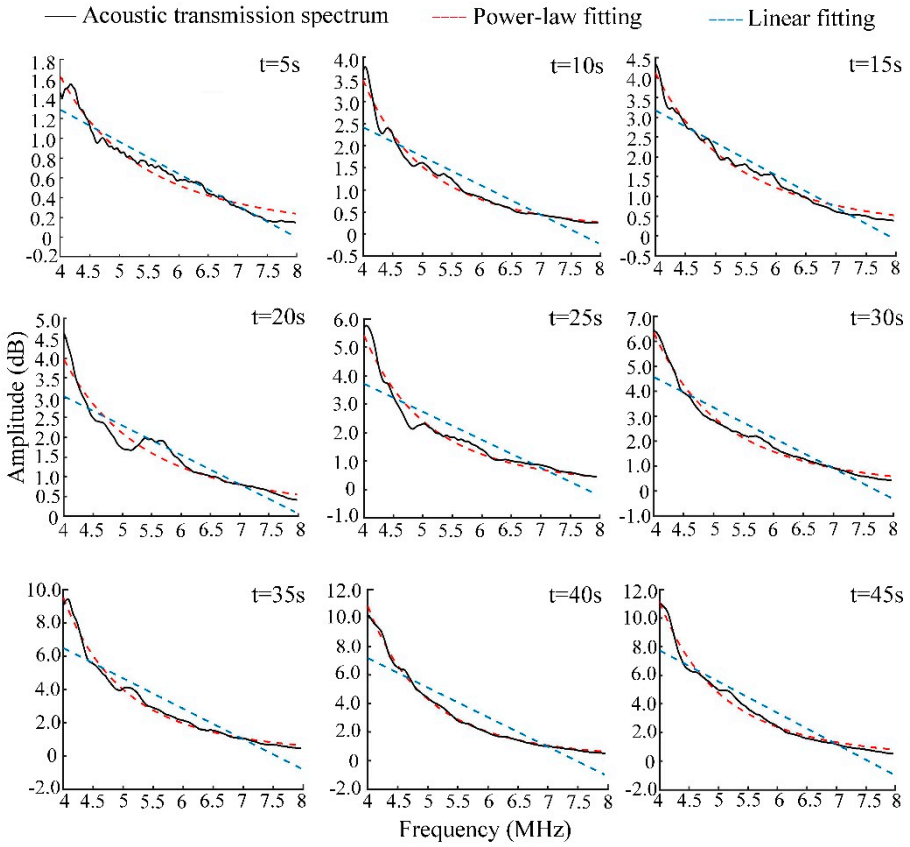


Figure 2. ATS of volunteer 1 every 5 s during the SC process.

3. Results

3.1. MVC Force and MET of Each Subject

The results of the three tests of MVC force are given in Table 1. The max values of the three tests were chosen as the MVC force.

Table 1. Maximal voluntary contraction (MVC) force of each volunteer (/N).

Volunteer	1	2	3	4	5	6	7	8	9
Test 1	20.0	18.5	16.2	15.6	16.0	15.5	14.2	13.9	13.4
Test 2	19.8	18.3	16.5	15.8	15.6	16.0	14.5	14.0	13.5
Test 3	19.6	18.0	16.0	16.0	15.8	15.3	14.3	13.5	13.0
Max value	20.0	18.5	16.5	16.0	16.0	16.0	14.5	14.0	13.5

Table 2 shows the METs of each volunteer. The METs of the different volunteers are similar.

Table 2. Maximum endurance times (METs) of each volunteer under 60% MVC SC exercise (/s).

Volunteer	1	2	3	4	5	6	7	8	9	Mean Value	SD
MET	45.0	46.0	50.0	52.0	51.0	50.0	53.0	48.0	46.0	49.0	2.9

3.2. Ultrasound Image Entropy

Previous studies revealed that the image entropy of the B-ultrasound image decreases with muscle fatigue [14]. Thus, we calculated the ultrasound image entropy (USIE) of each volunteer during the SC test and proved that the muscles in this study underwent a fatigue

process. Taking volunteer 1 as a case, the center part of the muscle layer is chosen as the region of interest (ROI) in Figure 3, and the corresponding USIEs are calculated. Linear fits were used to analyze the variability of the USIEs. The USIEs of each volunteer in Figure 4 showed a similar decrease during the SC test.

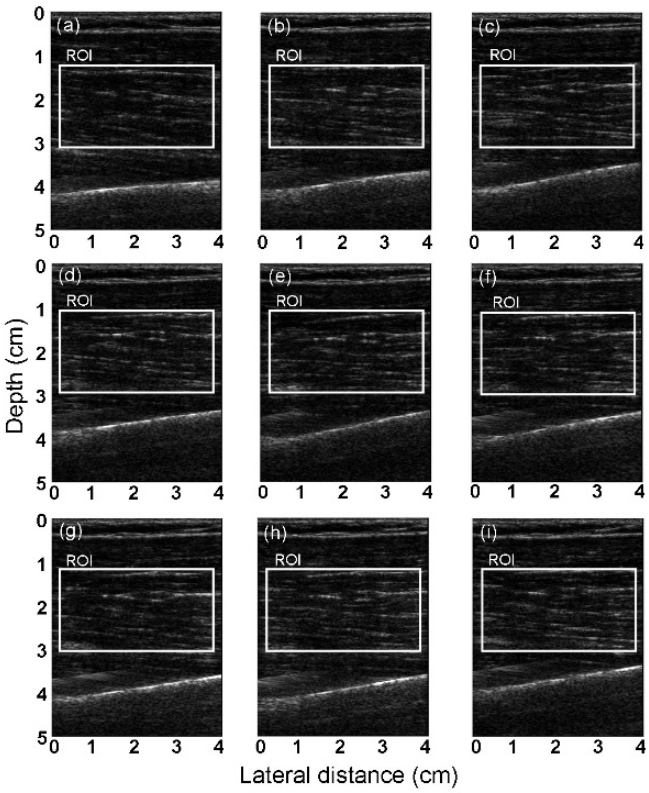


Figure 3. (**a**–**i**) B-ultrasound images of volunteer 1 every 5 s during the SC process.

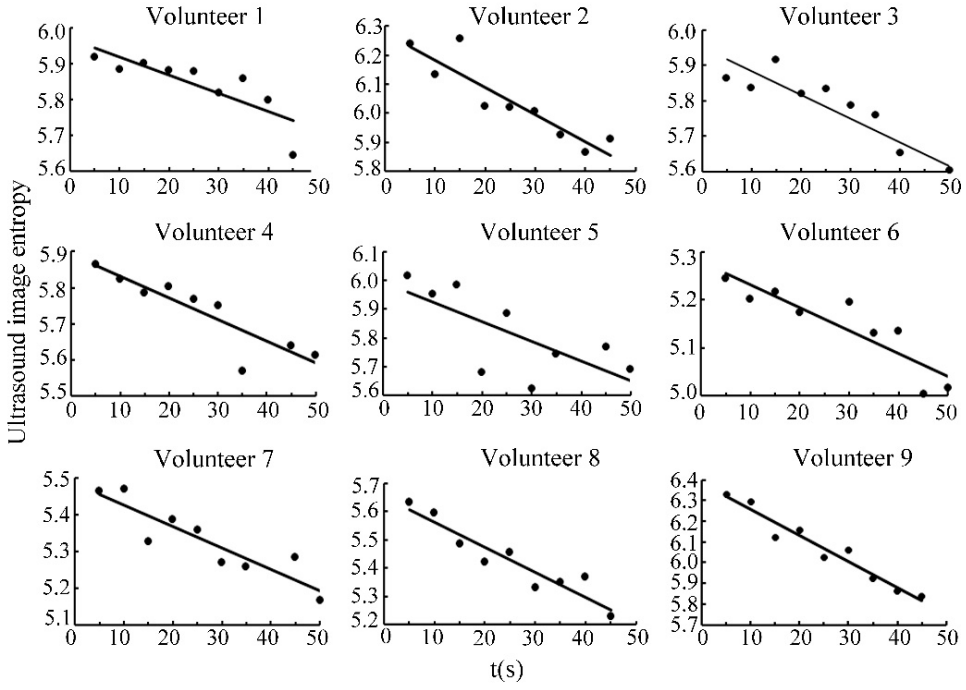


Figure 4. USIEs of each volunteer during the SC process.

3.3. Fitting Coefficients of ATS during Fatigue Process

Depending on the two fitting models, we calculated the coefficients a, b, α, and β of ATS along with the SC process, and drew the coefficients of volunteers with similar MVC forces in one figure, as shown in Figure 5. The slope a decreases linearly, and the intercept b increases linearly; the α increases exponentially, and the β decreases linearly along with the duration of SC of each volunteer. For the volunteers with similar MVC forces, their a, b, and α vary similarly along fatigue.

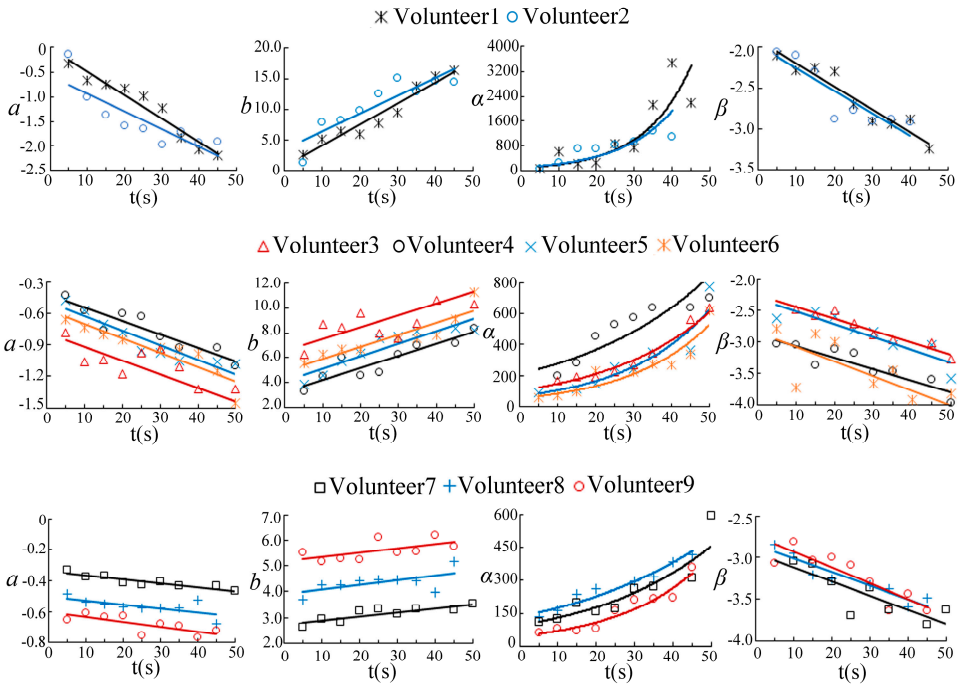


Figure 5. Changes in coefficients a, b, α, and β of each volunteer during the SC process.

4. Analyses and Discussion

The decrease in USIEs indicated that all volunteers experienced a muscle fatigue process along with the SC tests and the scattering properties of the myofiber changes [14]. The viscous absorption and interface scattering are dominant reasons for acoustic attenuation in human skeletal muscles [29]; these two physical processes are all frequency dependent. Therefore, we analyzed the variation of ATS based on the coefficients a, b, α, and β of two fitting models along with the fatigue process.

4.1. Variations of ATS during Fatigue Process

A review on skeletal muscle fatigue [3] reported that increased metabolites during sustained isometric contraction contribute to muscle fatigue. Zhang et al. [20] studied the interstitial fluid (IF) metabolomics of adults at rest and during exercise. They found that the IF concentrations were also increased for $\geq$12 amino acids after exercise. The accumulation of metabolites and intracellular fluid during muscle contraction may reduce the gap between the muscle fibers, which is beneficial for acoustic transmission. On the other hand, voluntary maximal isometric contraction will increase muscle viscosity [30].

Place et al. [4] pointed out that most of the peripheral impairment induced by sustained submaximal isometric contractions is located within the muscle fibers. In the downhill running sports models of rats [31], researchers found that the ultrastructure of muscle changed: the myofilament arrangement appeared disordered, even disrupted. Changes in myofibrils enables smaller impedance interfaces for acoustic scattering in skeletal muscles. Theoretically, as the scatter becomes smaller, the scattering of low-frequency waves will be weaker, while the scattering of high-frequency waves will change slightly.

The larger the absolute value of a, the larger the amplitude difference between low- and high-frequency components will be. The larger b indicates an increase in the low-frequency amplitude. The larger α means an increase in the total acoustic energy. The larger absolute value of β indicates the larger amplitude difference between low- and high-frequency components. In addition, the ATS in Figure 2 shows similar results during the fatigue process, the amplitude of low-frequency components increases continuously, and the amplitude of high-frequency components does not change significantly, hence the total acoustic energy increase. A comprehensive analysis of all four parameters could better represent the ATS of the muscle.

4.2. Relationship between MVC Force and Muscle Fatigue

To characterize the magnitude of the ATS variation, we subtract the values of these coefficients at the end of the SC process from those at the beginning, as shown in Table 3. Δa, Δb, $\Delta \alpha$, and $\Delta \beta$ show high dependence on the MVC force. They are larger for volunteers with larger MVC forces and similar for volunteers with similar MVC forces. According to the exercise procedure, volunteers with higher MVC forces will experience higher SC intensity. Hence, higher exercise intensity may induce larger changes in the physiological properties of skeletal muscles, which then affect the ATS. Variations of these coefficients could be valuable for assessing exercise intensity.

Table 3. Variation magnitudes of a, b, α, and β during the fatigue process.

Subject	MVC Force (N)	Variation Magnitude of the Coefficients			
		$\Delta\alpha$	$\Delta\beta$	Δa	Δb
1	20.0	2118.85	−1.15	−1.86	13.89
2	18.5	1418.44	−1.14	−1.77	13.32
3	16.5	453.00	−0.70	−0.53	4.01
4	16.0	498.60	−0.94	−0.67	5.14
5	16.0	614.20	−0.95	−0.61	4.38
6	16.0	558.76	−1.03	−0.80	5.75
7	14.5	382.90	−0.58	−0.14	0.90
8	14.0	280.20	−0.65	−0.19	1.46
9	13.5	297.20	−0.57	−0.12	0.61

4.3. Limitations and Future Work

Nine healthy male subjects were recruited in this study. Previous studies have shown that muscle fatigue between males and females, younger and older, have significant differences [32]. In different exercise modes, the mechanism of fatigue is also significantly different [33]. Therefore, future work needs to increase the experimental sample size, including different ages, genders, and different exercise modes and intensities. In addition, we only analyzed the spectrum changes in the RF echo signal during the fatigue process. It would be meaningful to explore the other parameters of the RF echo signal.

Based on ultrasound images, muscle changes such as the thickness, pennate angle, and fascicle length can be analyzed with muscle fatigue [12,13]. The ultrasonic image entropy can reflect the textural features and microstructure changes with muscle fatigue [14,15]. The ultrasound echo signal can not only reflect the structure of the muscle, but can also carry a large amount of organizational information along its path. Therefore, ATS may be a sensitive modality to characterize the ultrastructural and interstitial fluid changes of muscle and could have great potential in evaluating muscle fatigue nondestructively.

5. Conclusions

This study investigated variations in ATS during muscle fatigue. The ATS of the muscle was obtained and fitted using the linear and power-law models. As muscle fatigue increases, the intensity of the low-frequency waves increases, the total acoustic energy increases, and the difference between the low- and high-frequency intensity increases. Moreover, we find that the fatigue process is highly dependent on the strength of the exercise. The larger the strength of the exercise, the more the ATS varies. These results suggest that a comprehensive analysis of ATS is a potential metric for assessing muscle fatigue. Moreover, as ATS carry the structural and mechanical properties of muscles, we believe it is a potential method with unique value to investigate the ultrastructural and interstitial fluid changes during muscle fatigue nondestructively.

Author Contributions: Conceptualization, P.L. and G.Y.; software, S.N.; validation, P.L. and S.N.; formal analysis, P.L.; investigation, P.L. and G.Y.; resources, J.G.; data curation, P.L. and S.N.; writing—original draft preparation, P.L. and G.Y.; writing—review and editing, P.L. and G.Y.; visualization, P.L.; supervision, G.Y. and J.G.; project administration, G.Y. and J.G.; funding acquisition, G.Y. and J.G. All authors have read and agreed to the published version of the manuscript.

Funding: This research was funded by the National Natural Science Foundation of China (grant numbers 12004237, 11727813, and 12034005), the China Postdoctoral Science Foundation (Grant No. 2020M683416), and the Young Talent Fund of Association for Science and Technology in Shaanxi, China (Grant No. 20220523).

Institutional Review Board Statement: The study was conducted in accordance with the Declaration of Helsinki and approved by the Ethics committee of Shaanxi Normal University.

Informed Consent Statement: Informed consent was obtained from all subjects involved in the study.

Data Availability Statement: The datasets analyzed during the current study are available from the corresponding author on reasonable request.

Acknowledgments: The authors would like to thank the Key Laboratory of Shaanxi Province and all the volunteers in this study from the School of Physics and Information Technology for all of the support during the data collection.

Conflicts of Interest: The authors declare no conflict of interest.

References

1. Wan, J.J.; Qin, Z.; Wang, P.Y.; Sun, Y.; Liu, X. Muscle fatigue: General understanding and treatment. *Exp. Mol. Med.* **2017**, *49*, 384. [CrossRef]
2. Harrington, M.E. Neurobiological studies of fatigue. *Prog. Neurobiol.* **2012**, *99*, 93–105. [CrossRef] [PubMed]
3. Allen, D.G.; Lamb, G.D.; Westerblad, H. Skeletal muscle fatigue: Cellular mechanisms. *Physiol. Rev.* **2008**, *88*, 287–332. [CrossRef] [PubMed]
4. Place, N.; Bruton, J.D.; Westerblad, H. Mechanisms of fatigue induced by isometric contractions in exercising humans and in mouse isolated single muscle fibres. *Clin. Exp. Pharmacol. Physiol.* **2009**, *36*, 334–339. [CrossRef]
5. João, F.; Alves, S.; Secca, M.; Noseworthy, M.; Veloso, A. Fatigue Effects on the Lower Leg Muscle Architecture Using Diffusion Tensor MRI. *Appl. Sci.* **2020**, *12*, 9767. [CrossRef]
6. Goubault, E.; Etienne, F.; Pelletier, J.; Traube, C.; Begon, M.; Dal Maso, F. Exhausting repetitive piano tasks lead to local forearm manifestation of muscle fatigue and negatively affect musical parameters. *Sci. Rep.* **2021**, *11*, 8117. [CrossRef]
7. Akyildiz, Z.; Ocak, Y.; Clemente, F.M.; Birgonul, Y.; Günay, M.; Nobari, H. Monitoring the post-match neuromuscular fatigue of young Turkish football players. *Sci. Rep.* **2022**, *12*, 13835. [CrossRef]
8. Troiano, A.; Naddeo, F.; Sosso, E.; Camarota, G.; Merletti, R.; Mesin, L. Assessment of force and fatigue in isometric contractions of the upper trapezius muscle by surface EMG signal and perceived exertion scale. *Gait Posture* **2008**, *28*, 179–186. [CrossRef]
9. Mami, S.; Khaje, G.; Shahriari, A.; Gooraninejad, S. Evaluation of biological indicators of fatigue and muscle damage in arabian horses after race. *J. Equine. Vet. Sci.* **2019**, *78*, 74–78. [CrossRef]
10. Venugopal, G.; Navaneethakrishna, M.; Ramakrishnan, S. Extraction and analysis of multiple time window features associated with muscle fatigue conditions using sEMG signals. *Expert. Syst. Appl.* **2014**, *41*, 2652–2659. [CrossRef]
11. Matrone, G.; Ramalli, A.; Tortoli, P. Ultrasound B-Mode Imaging: Beamforming and Image Formation Techniques. *Appl. Sci.* **2019**, *9*, 2507. [CrossRef]

12. Shi, J.; Zheng, Y.P.; Chen, X.; Huang, Q.H. Assessment of muscle fatigue using sonomyography: Muscle thickness change detected from ultrasound images. *Med. Eng. Phys.* **2007**, *29*, 472–479. [CrossRef]
13. Zhou, G.Q.; Chan, P.; Zheng, Y.P. Automatic measurement of pennation angle and fascicle length of gastrocnemius muscles using real-time ultrasound imaging. *Ultrasonics* **2015**, *57*, 72–83. [CrossRef] [PubMed]
14. Li, P.; Yang, X.; Yin, G.; Guo, J. Skeletal muscle fatigue state evaluation with ultrasound image entropy. *Ultrason. Imaging* **2020**, *42*, 235–244. [CrossRef]
15. Taniguchi, M.; Yamada, Y.; Ichihashi, N. Acute effect of multiple sets of fatiguing resistance exercise on muscle thickness, echo intensity, and extracellular-to-intracellular water ratio. *Appl. Physiol. Nutr. Metab.* **2020**, *45*, 213–219. [CrossRef] [PubMed]
16. Weng, W.C.; Lin, C.W.; Shen, H.C.; Chang, C.C.; Tsui, P.H. Instantaneous frequency as a new approach for evaluating the clinical severity of Duchenne muscular dystrophy through ultrasound imaging. *Ultrasonics* **2019**, *94*, 235–241. [CrossRef] [PubMed]
17. Ament, W.; Verkerke, G.J. Exercise and fatigue. *Sport. Med.* **2009**, *39*, 389–422. [CrossRef]
18. Jones, D.A.; Rutherford, O.M.; Parker, D.F. Physiological changes in skeletal muscle as a result of strength training. *Q. J. Exp. Physiol.* **1989**, *74*, 233–256. [CrossRef]
19. Lauritzen, F.; Paulsen, G.; Raastad, T.; Bergersen, L.H.; Owe, S.G. Gross ultrastructural changes and necrotic fiber segments in elbow flexor muscles after maximal voluntary eccentric action in humans. *J. Appl. Physiol.* **2009**, *107*, 1923–1934. [CrossRef] [PubMed]
20. Zhang, J.; Bhattacharyya, S.; Hickner, R.C.; Light, A.R.; Lambert, C.J.; Gale, B.K.; Adams, S.H. Skeletal muscle interstitial fluid metabolomics at rest and associated with an exercise bout: Application in rats and humans. *Am. J. Physiol. Metab.* **2019**, *316*, 43–53. [CrossRef]
21. Lizzi, F.L.; Ostromogilsky, M.; Feleppa, E.J.; Rorke, M.C.; Yaremko, M.M. Relationship of ultrasonic spectral parameters to features of tissue microstructure. *IEEE Trans. Ultrason. Ferroelectr. Freq. Control.* **1987**, *34*, 319–329. [CrossRef] [PubMed]
22. Lizzi, F.L.; Greenebanm, M.; Feleppa, E.J.; Elbaum, M.; Coleman, D.J. Theoretical framework for spectrum analysis in ultrasonic tissue characterization. *J. Acoust. Soc. Am.* **1983**, *73*, 1366–1373. [CrossRef]
23. Moradi, M.; Mousavi, P.; Abolmaesumi, P. Computer-aided diagnosis of prostate cancer with emphasis on ultrasound-based approaches: A review. *Ultrasound Med. Biol.* **2007**, *33*, 1010–1028. [CrossRef]
24. Liu, T.; Lizzi, F.L.; Silverman, R.H.; Kutcher, G.J. Ultrasonic tissue characterization using 2-D spectrum analysis and its application in ocular tumor diagnosis. *Med. Phys.* **2004**, *31*, 1032–1039. [CrossRef] [PubMed]
25. Lang, M.; Ermert, H.; Heuser, L. In vivo study of online liver tissue classification based on envelope power spectrum analysis. *Ultrason. Imaging* **1994**, *16*, 77–86. [CrossRef]
26. Fry, N.R.; Gough, M.; Shortland, A.P. Three-dimensional realisation of muscle morphology and architecture using ultrasound. *Gait Posture* **2004**, *20*, 177–182. [CrossRef]
27. Shan, X.; Otsuka, S.; Li, L.; Kawakami, Y. Inhomogeneous and anisotropic mechanical properties of the triceps surae muscles and aponeuroses in vivo during submaximal muscle contraction. *J. Biomech.* **2021**, *121*, 110396. [CrossRef]
28. Li, A.; Zhou, J.; Lin, C.; Chen, Y. Ultrasonic Spectrum Analysis for In Vivo Characterization of Tumor Microstructure Changes After Chemotherapy in a Murine Breast Cancer Model. *Ultrasound Med. Biol.* **2013**, *39*, 65. [CrossRef]
29. Nassiri, D.K.; Nicholas, D.; Hill, C.R. Attenuation of ultrasound in skeletal muscle. *Ultrasonics* **1979**, *17*, 230–232. [CrossRef]
30. Chalchat, E.; Gennisson, J.L.; Peñailillo, L.; Oger, M.; Malgoyre, A.; Charlot, K.; Garcia-Vicencio, S. Changes in the viscoelastic properties of the vastus lateralis muscle with fatigue. *Front. Physiol.* **2020**, *11*, 307. [CrossRef] [PubMed]
31. Ying, J.; Cen, X.; Yu, P. Effects of eccentric exercise on skeletal muscle injury: From an ultrastructure aspect: A review. *Phys. Act. Health* **2021**, *5*, 15–20. [CrossRef]
32. Lindström, B.; Lexell, J.; Gerdle, B.; Downham, D. Skeletal muscle fatigue and endurance in young and old men and women. *J. Gerontol. A Bol.* **1997**, *52*, 59–66. [CrossRef] [PubMed]
33. Kent-Braun, J.A.; Fitts, R.H.; Christie, A. Skeletal muscle fatigue. *Compr. Physiol.* **2011**, *2*, 997–1044.

Disclaimer/Publisher's Note: The statements, opinions and data contained in all publications are solely those of the individual author(s) and contributor(s) and not of MDPI and/or the editor(s). MDPI and/or the editor(s) disclaim responsibility for any injury to people or property resulting from any ideas, methods, instructions or products referred to in the content.